Generation of Triarylamine Radical Cations through Reaction of Triarylamines with Cu(II) in Acetonitrile. A Kinetic Investigation of the Electron-Transfer Reaction

Kesavapillai Sreenath,[†] Chettiyam Veettil Suneesh,[†] Karical R. Gopidas,[*,†] and Robert A. Flowers II[*,‡]

Photosciences and Photonics, Chemical Sciences and Technology Division, National Institute for Interdisciplinary Science and Technology (NIIST), Council of Scientific and Industrial Research (CSIR), Trivandrum 695 019, India, and Department of Chemistry, Lehigh University, Bethlehem, Pennsylvania 18015-3172

Received: March 26, 2009

Triphenylamine derivatives react with Cu^{2+} in acetonitrile to give radical cations, which subsequently undergo dimerization to provide tetraphenylbenzidine derivatives. Kinetic aspects of radical cation formation were examined by stopped-flow spectrophotometry. A broad range of triphenylamine derivatives were studied, and the driving force for the electron-transfer reaction ranged from +3.67 to −8.56 kcal M^{-1} with rate constants varying from 1.09×10^2 to 2.15×10^5 M^{-1} s^{-1} for these systems. Reorganization energy for the electron-transfer reaction was estimated using experimentally determined activation parameters. Fitting of the rate data to the Marcus equation using different values of the electronic coupling matrix element H_{el} provided a good fit with $H_{el} = 100$ cm^{-1} suggesting that electron transfer in the TPA/Cu^{2+} system conforms to the Marcus-type electron transfer. Furthermore, the high reorganization obtained from these studies is consistent with significant bond cleavage in the transition state, and a mechanism consistent with the experimental data is proposed.

1. Introduction

Amine radical cations are principal intermediates in several single electron-transfer reactions.[1−3] They are also important intermediates in technological applications such as imaging and photopolymerization.[4,5] Several methods are now available to generate amine radical cations and study their properties. Most important among these is the anodic oxidation of amines in polar solvents such as acetonitrile.[6−8] Other methods include treatment of the amine substrates with oxidizing metals, Lewis acids, protic acids, and onium salts.[9] Photoionization[10] and inclusion in zeolite cavities[11,12] are also known to generate amine radical cations. In most of these cases, mechanistic and kinetic aspects of radical cation formation are not explored. Dependence of the reaction rate on important factors such as oxidation potential of the amine is also not studied.

Recently, we observed that radical cations of aromatic amines can be prepared easily by the reaction of precursor amines with copper(II) perchlorate in acetonitrile (ACN).[13−15] For example, several triphenylamine (TPA) derivatives reacted with Cu^{2+} in acetonitrile to give radical cations ($TPA^{\bullet+}$) as shown in Scheme 1.

$TPA^{\bullet+}$ formed underwent dimerization to give tetraphenylbenzidines (TPB) in very good yields, and the Cu^{+} generated was converted to the stable tetrakis(acetonitrile)copper(I) complex ($[Cu(ACN)_4]^+$). Although Scheme 1 is consistent with electron transfer from TPA to Cu^{2+}, the mechanistic details of these reactions were not known. Our investigations now show that for several TPA derivatives the rates of radical cation formation could be measured using stopped-flow spectrophotometry, and results of this study are presented here. We are interested in developing an understanding of the measured rate constants and activation parameters in terms of the elementary steps of a model outer-sphere electron-transfer mechanism. As a consequence, a major objective of the study was to correlate the activation parameters obtained from the kinetic studies to the free energy change associated with the reaction and to determine if the reaction conforms to the Marcus theory of electron transfer. We anticipated that the kinetic investigations would provide a better understanding of the mechanistic aspects of this electron-transfer reaction. Recent years have seen considerable efforts to analyze several organic reactions in terms of established electron-transfer theories, and the present work is also an attempt in that direction.[16−21]

2. Experimental Section

TPA derivatives **1−8** were synthesized according to literature procedures.[15] Copper(II) perchlorate was purchased from Aldrich. Spectroscopic grade acetonitrile was used for the kinetic investigations. The electronic absorption spectra were recorded on a Shimadzu 3101PC UV−vis−NIR (near-infrared) scanning spectrophotometer. Redox potentials of the TPA derivatives were recorded using a BAS CV50W voltammetric analyzer. Solutions of the TPA derivatives (1×10^{-3} M) in acetonitrile containing 0.1 M tetra-*n*-butylammonium hexafluorophosphate as supporting electrolyte were thoroughly deaerated before use. A glassy carbon electrode was used as the working electrode, a platinum wire was used as counter electrode, and the potentials were referenced to SCE. Kinetic experiments were performed with a computer controlled SX 18 MV stopped-flow spectrophotometer (Applied Photophysics). Temperature dependence studies were carried out over a range between 15 and 50 °C using a Neslab circulator connected to the sample-handling unit of the stopped-flow reaction analyzer. The step size used for

* To whom correspondence should be addressed. E-mail: gopidaskr@rediffmail.com (K.R.G.); rof2@Lehigh.EDU (R.A.F.).
[†] National Institute for Interdisciplinary Science and Technology.
[‡] Lehigh University.

10.1021/jp9027222 CCC: $40.75
Published on Web 05/19/2009

SCHEME 1: Scheme for the Generation and Reaction of $TPA^{•+}$

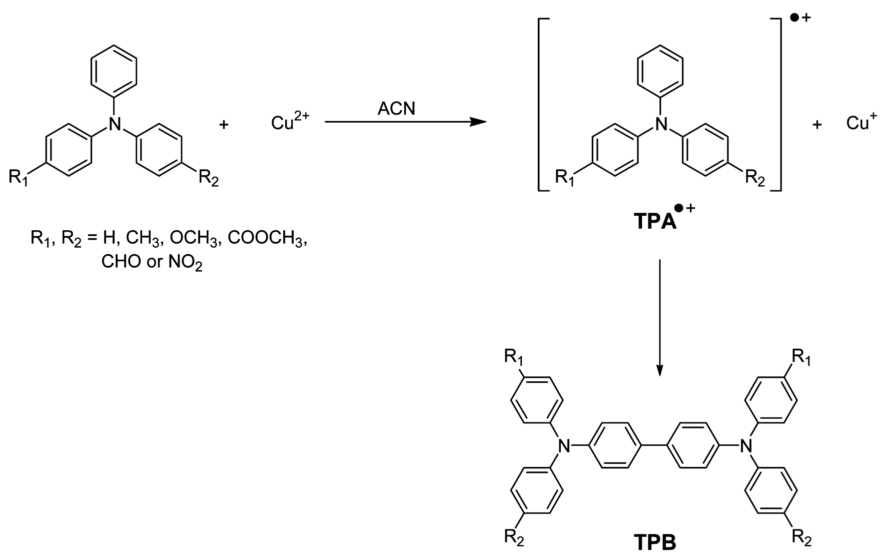

TABLE 1: TPA Derivatives, Their Oxidation Potentials, ΔG^0 Values, and Absorption Maxima of $TPA^{•+}$

Compound Number	Structure	E_{ox}, V vs SCE	ΔG^0, kcal M^{-1}	$\lambda_{TPA^{•+}}$, nm
1	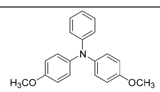	+ 0.63	- 8.56	737
2	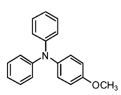	+ 0.76	- 5.56	695
3	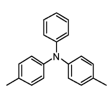	+ 0.88	- 2.80	671
4	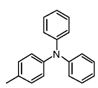	+ 0.90	- 2.33	669
5	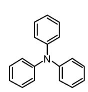	+ 0.92	- 1.87	679
6	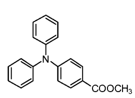	+ 1.05	+ 1.13	670
7	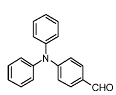	+ 1.08	+ 1.82	675
8	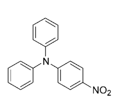	+ 1.16	+ 3.67	656

the temperature study was 5 °C, and each kinetic trace was recorded at a known temperature that was measured by a thermocouple in the reaction cell.

3. Results and Discussion

Structures of the TPA derivatives (**1**−**8**) studied are shown in Table 1. Mixing the TPA derivatives with $Cu(ClO_4)_2 \cdot 6H_2O$ in acetonitrile results in the formation of a deep blue color indicative of the formation of $TPA^{•+}$. An example is given in Figure 1, which shows the absorption spectra of **1** in the absence and presence (immediately after mixing) of 1 equiv of Cu^{2+}. The strong band formed at 737 nm in the presence of Cu^{2+} is assigned to the radical cation ($\mathbf{1}^{•+}$) based on literature reports and our own previous studies.[15]

For all the TPA derivatives studied, radical cation absorption maxima ($\lambda_{TPA^{•+}}$) were observed in the 650−730 nm region (Table 1). Formation of radical cations $\mathbf{1}^{•+}$−$\mathbf{8}^{•+}$ in these reactions was also confirmed by observation of their EPR (electron paramagnetic resonance) spectra.[15] Since an electron transfer is involved in the reaction in Scheme 1, the free energy change ΔG^0 for this process could be calculated using the standard expression

$$\Delta G^0 = E_{ox} - E_{red} - e^2/d\varepsilon_s \qquad (1)$$

where E_{ox} is the oxidation potential of the TPA derivative, E_{red} is the reduction potential of the Cu^{2+}, d is the center-to-center distance between TPA and $Cu(ClO_4)_2$ hexahydrate in the collision complex, and ε_s is the dielectric constant of ACN. E_{ox} values for all the TPA derivatives were measured in ACN using cyclic voltammetry (Table 1). The Coulombic term in eq 2 was calculated assuming d = 8 Å. Using these values, the ΔG^0 associated with $TPA^{•+}$ formation were calculated for all TPA derivatives, and these values are presented in Table 1. For the series of TPA derivatives **1**−**8** listed in Table 1, ΔG^0 values varied from −8.56 to +3.67 kcal M^{-1}. For TPAs **1**−**5**, ΔG^0 values are negative, and the reactions are exergonic. For TPAs

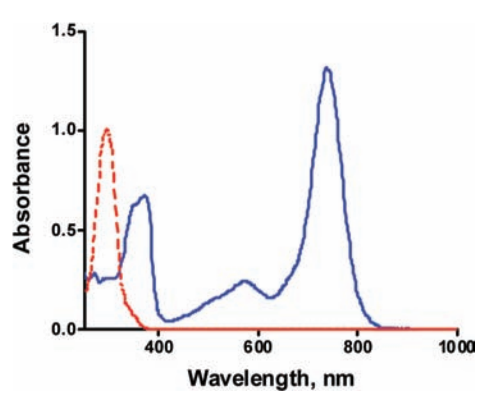

Figure 1. Absorption spectra of **1** (5×10^{-5} M) in the absence (---) and presence (—) of $Cu(ClO_4)_2 \cdot 6H_2O$ (5×10^{-5} M) in acetonitrile.

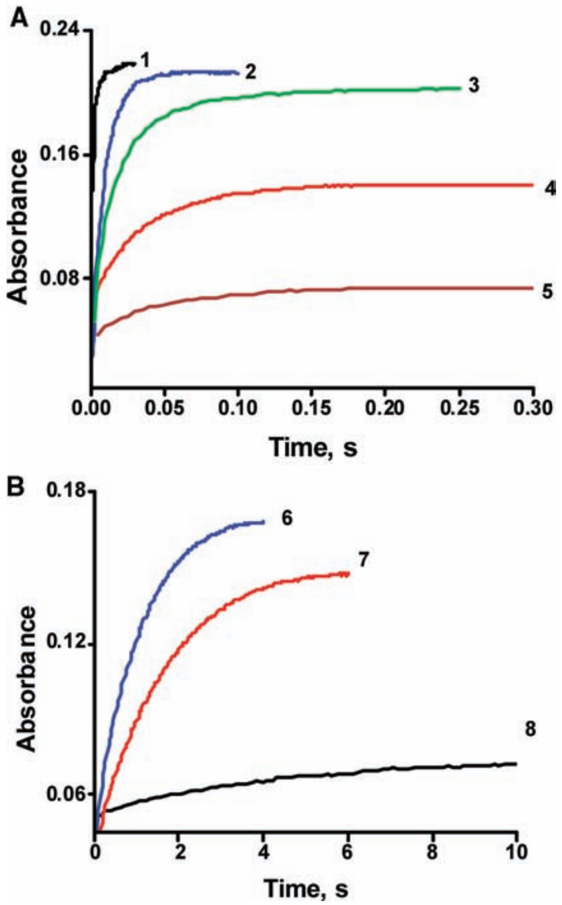

Figure 2. (A) Absorbance−time profile for the formation of $TPA^{\bullet+}$ from **1** to **5** (20×10^{-4} M) and $Cu(ClO_4)_2 \cdot 6H_2O$ (1×10^{-4} M) in ACN. (B) Absorbance−time profile for the formation of $TPA^{\bullet+}$ from **6** to **8** (20×10^{-4} M) and $Cu(ClO_4)_2 \cdot 6H_2O$ (1×10^{-4} M) in ACN.

6−**9**, where the molecules contain electron withdrawing substituents, ΔG^0 values were positive. For all these systems, radical cation formations were observed in the 600−800 nm region, and these absorptions could be monitored by the stopped-flow technique to obtain the kinetic information reported here.

Formation of the radical cations for all TPA derivatives was studied using stopped-flow spectrophotometry. The rate of $TPA^{\bullet+}$ formation was dependent on the ΔG^0 value and was fastest for **1** and slowest for **8**, as shown in Figure 2A,B.

In addition to TPA systems shown in Table 1, the radical cation formation for tris(4-methoxyphenyl)amine ($E_{ox} = +0.52$ V, $\Delta G^0 = -11.1$ kcal M^{-1}) and di(4-nitrophenyl)phenylamine ($E_{ox} = +1.35$ V, $\Delta G^0 = +8.05$ kcal M^{-1}) was also investigated under the same conditions. Formation of the radical cation was too fast for the former and too slow for the latter, and these systems could not be studied. Figure 2 reveals that, for the dimethoxy derivative **1**, radical cation formation was complete within 30 ms, whereas for the nitro derivative **8** radical cation formation was not complete even at 10 s.

In order to obtain rate constants of the electron-transfer reaction, stopped flow experiments were performed under pseudo-first-order conditions ($[TPA] > 20 \times [Cu^{2+}]$). Growths of the $TPA^{\bullet+}$ absorptions were exponential under these conditions. The growth profiles were fit to a first-order kinetic equation to obtain observed rate constants. ($k_{obs} = k_{et}[TPA]$, where k_{et} is the bimolecular electron-transfer rate constant.) To obtain k_{et} values, the k_{obs} values were determined at different concentrations of TPA and plotted against [TPA] as shown in Figure 3. Straight lines were obtained for all systems, and k_{et} values were obtained from the slopes of these plots. The k_{et} values obtained varied from 1.09×10^2 M^{-1} s^{-1} for **8** to 2.15×10^5 M^{-1} s^{-1} for **1** as shown in Table 2.

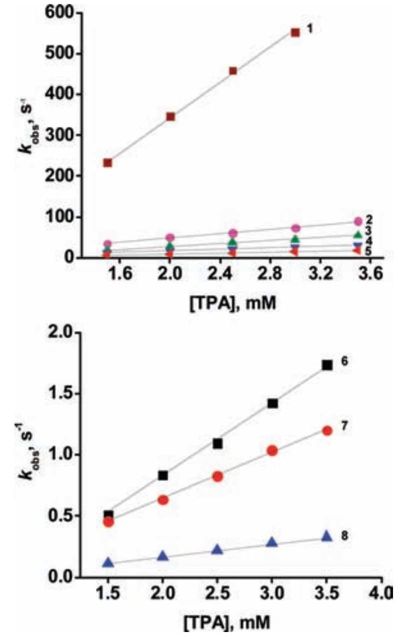

Figure 3. Plots of the pseudo-first-order rate constants vs TPA concentration for TPA derivatives **1**−**8**.

TABLE 2: Rate Constants and Activation Parameters for the Electron Transfer between TPA and Cu^{2+} in ACN

TPA	k_{et},[a] M^{-1} s^{-1}	$\Delta H^{\#}$, kcal M^{-1}	$\Delta S^{\#}$, kcal M^{-1} K^{-1}	$\Delta G^{\#}$, kcal M^{-1}	E_a, kcal M^{-1}	ΔG^*, kcal M^{-1}
1	214560 ± 6644	6.36	−0.024	13.98	6.96	6.66
2	26638 ± 1210	8.90	−0.019	14.61	9.50	9.20
3	16934 ± 413	11.04	−0.015	15.38	11.63	11.33
4	9282 ± 241	11.83	−0.013	15.67	12.42	12.12
5	5960 ± 357	12.63	−0.005	15.90	13.22	12.92
6	608 ± 20	14.55	−0.010	17.47	15.14	14.84
7	376 ± 7	15.64	−0.003	17.68	16.23	15.93
8	109 ± 2	16.90	−0.008	18.47	17.50	17.20

[a] Experimental values are reported as $\pm\sigma$.

SCHEME 2: Kinetic Scheme for $TPA^{\bullet+}$ Formation

$TPA + Cu^{2+} \xrightarrow{k_1} (TPA:Cu^{2+})$		**reactant encounter**
$(TPA:Cu^{2+}) \xrightarrow{k_{-1}} TPA + Cu^{2+}$		**reactant separation**
$(TPA:Cu^{2+}) \xrightarrow{k_2} \{TPA^{\bullet+} + Cu^{+}\}$		**ET in encounter pair**
$\{TPA^{\bullet+} + Cu^{+}\} \xrightarrow{k_{-2}} (TPA:Cu^{2+})$		**reverse ET**
$\{TPA^{\bullet+} + Cu^{+}\} \xrightarrow{k_3}$ Products		**product separation**

To understand the reaction, probable elementary steps were considered to obtain a kinetic equation. Since electron transfer between TPA and Cu^{2+} is a bimolecular reaction, it would involve steps such as formation of the encounter complex, reactant separation, electron transfer within the encounter complex, reverse electron transfer, and product separation as shown in Scheme 2.

The assumption of steady-state conditions for $(TPA:Cu^{2+})$ and $\{TPA^{\bullet+} + Cu^{+}\}$leads to the following equation.[22,23]

$$-d[TPA]/dt = k_{et}[TPA][Cu^{2+}] \quad (2)$$

where

$$k_{et} = \{(k_1/k_{-1})(k_2/k_{-2})k_3\}/[1 + (k_3/k_{-2}) + (k_2k_3/k_{-1}k_{-2})] \quad (3)$$

If we assume that $k_3 \gg k_{-2}$, then $k_3/k_{-2} \gg 1$, and the equation reduces to

$$k_{et} = \{(k_1/k_{-1})(k_2/k_{-2})k_3\}/[(k_3/k_{-2}) + (k_2k_3/k_{-1}k_{-2})] \quad (4)$$

If we further assume that $k_{-1} \gg k_2$, the equation further reduces to

$$k_{et} = (k_1/k_{-1})k_2 \quad (5)$$

$(k_1/k_{-1}) = K_d$, the equilibrium constant for encounter pair formation. Thus, the observed second-order rate constant for the electron-transfer reaction is the product of the equilibrium constant for encounter pair formation and the rate constant for electron transfer. Usually, $k_1 \sim k_{-1}$ and, hence, $K_d \sim 1$ M^{-1}. In the derivation above, two assumptions were made whose validity needs to be examined. The products of electron transfer, namely, $TPA^{\bullet+}$ and Cu^+, are both positively charged and repel each other thereby facilitating product separation leading to a high value for k_3. For TPA derivatives **1**−**5**, the free energy change for the reverse electron-transfer process will be positive which results in small k_{-2} values. Both factors support our assumption that $k_3 \gg k_{-2}$. Since the observed rate constants are well below the diffusion limit, the second assumption is also reasonable.

According to the activated complex theory, k_2 is given by

$$k_2 = (k_BT/h)\exp(-\Delta G^{\#}/RT) \quad (6)$$

where k_B is the Boltzmann constant, T is the temperature, h is Planck's constant (k_BT/h represents the frequency with which the activated complex crosses over to products), and $\Delta G^{\#}$ is the free energy of activation. ($\Delta G^{\#} = \Delta H^{\#} - T\Delta S^{\#}$, where $\Delta H^{\#}$ and $\Delta S^{\#}$ are the enthalpy and entropy of activation, respectively. Since the reactants are not charged, work terms can be neglected.) Substituting into eq 5 provides

$$k_{et} = K_d(k_BT/h)\exp(-\Delta G^{\#}/RT) \quad (7)$$

If we assume that K_d is temperature independent, the activation parameters can be determined by studying the temperature dependence of k_{et}. For all the TPA/Cu^{2+} systems, k_{obs} values were obtained at different temperatures, and the data were plotted using the linear form of the Eyring equation (8).[24,25]

$$\ln(k_{obs}h/k_BT) = -\Delta H^{\#}/RT + \Delta S^{\#}/R \quad (8)$$

Plots of $\ln(k_{obs}h/k_BT)$ vs $1/T$ for all the systems studied are shown in Figure 4. For the dimethoxy derivative **1**, radical cation formation was too fast at temperatures above 310 K. Hence, this system was studied in the range of 288−303 K. Other systems were studied in the range of 298−323 K. From the slopes and intercepts of these plots, $\Delta H^{\#}$ and $\Delta S^{\#}$ values were obtained. Using these values, the free energy of activation ($\Delta G^{\#} = \Delta H^{\#} - T\Delta S^{\#}$) and energy of activation ($E_a = \Delta H^{\#} + RT$) were also obtained. These values are presented in Table 2 along with the observed k_{et} values.

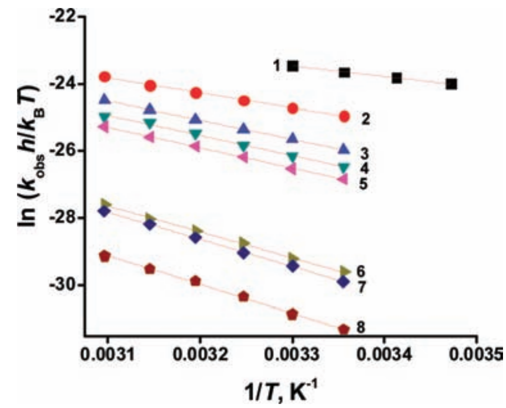

Figure 4. Eyring plots for all TPA/Cu^{2+} systems in ACN.

In the Marcus formalism of electron transfer based on reactive collisions, the rate constant for electron transfer is written as

$$k_2 = Z\exp(-\Delta G^*/RT) \quad (9)$$

where Z is the collision rate and ΔG^* is the Marcus free energy of activation.[26−28] Because of the different formulations, the Marcus free energy of activation differs from the activation energy E_a. These quantities are related as shown in eq 10.

$$E_a = \Delta G^* + RT/2 \quad (10)$$

Values for ΔG^* were calculated using eq 10, and these are also given in Table 2.

According to Marcus theory, ΔG^* is given by

$$\Delta G^* = (\Delta G^0 + \lambda)^2/4\lambda \quad (11)$$

where λ is the reorganization energy needed for the electron-transfer reaction.[26−28] λ is a combination of (i) internal reorganization energy (λ_i) arising out of changes in bond lengths and bond angles and (ii) solvent reorganization energy (λ_s) arising from the changes in the solvent shell surrounding the redox species.

For the TPA/Cu^{2+} reactions studied here, $|\Delta G^0|$ values are small. For a series of similar ET (electron transfer) reactions, if $|\Delta G^0/\lambda|$ is small, eqs 9 and 11 suggest that a plot of $k_BT \ln k_{et}$ vs $-\Delta G^0$ will be linear with a slope equal to $^1/_2$.[29−31] In Figure 5, $k_BT \ln k_{et}$ values are plotted against $-\Delta G^0$ along with a theoretical line with slope = $^1/_2$. The first six experimental points fall on the line indicating that eqs 9 and 11 hold good for the TPA/Cu^{2+} reaction. This confirms that these reactions follow the Marcus equation for outer-sphere electron transfer. For the last two systems, the assumption $|\Delta G^0/\lambda|$ may not be valid and results in the observed deviation.

The experimental data were further analyzed using the semiclassical Marcus equation,

$$k_2 = (2\pi/\hbar)(H_{el})^2(4\pi\lambda k_BT)^{-1/2}\exp[-(\Delta G^0 + \lambda)^2/4\lambda k_BT] \quad (12)$$

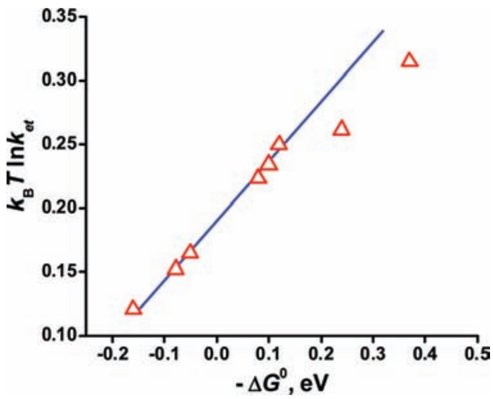

Figure 5. Plot of $k_B T \ln k_{et}$ vs $-\Delta G^0$ for the TPA/Cu^{2+} systems studied. A theoretical line with slope $^1/_2$ is also shown.

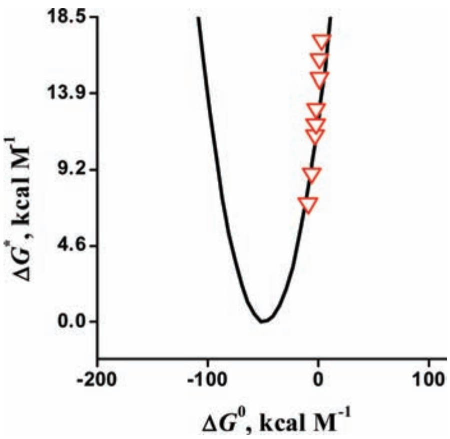

Figure 6. Plot of ΔG^* against ΔG^0 and theoretical fit using $\lambda = 48.43$ kcal M^{-1}.

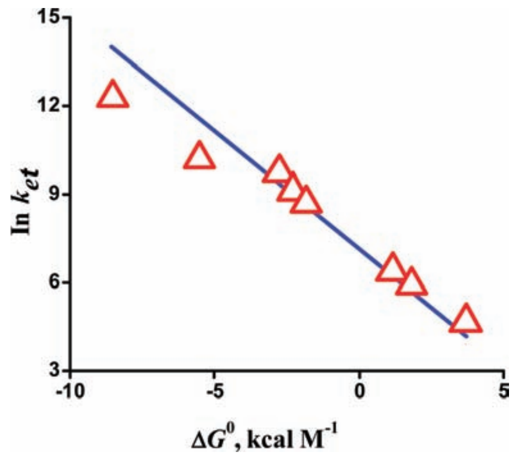

Figure 7. Plot of ln k_{et} vs ΔG^0 for the TPA/Cu^{2+} reaction. The solid line is a fit using $H_{el} = 100$ cm^{-1} and $\lambda = 48.43$ kcal M^{-1}.

where H_{el} is the donor–acceptor coupling element and $\hbar$ is Planck's constant divided by 2π. In order to compare the experimental k_{et} values with theoretical values from eq 12, H_{el} and λ values were required. These were obtained as follows.

For the TPA/Cu^{2+} systems examined here, ΔG^* varied from 6.66 kcal M^{-1} for **1** ($\Delta G^0 = -8.56$ kcal M^{-1}) to 17.20 kcal M^{-1} for **8** ($\Delta G^0 = +3.67$ kcal M^{-1}) as shown in Table 2. The ΔG^* values obtained were fit using eq 11 by employing different λ values. The data points along with the best fit (solid line) obtained using $\lambda = 48.43$ kcal M^{-1} are shown in Figure 6. This approach assumes that, for the series of TPA derivatives **1**–**8**, the electron-transfer reactions follow the same mechanism and that the reorganization energy λ is relatively constant in the series.

Using the λ values thus obtained, experimental k_{et} data were fit using eq 12 (substituted into eq 5) with $\lambda = 48.43$ kcal M^{-1} and different values of H_{el}. The best fit obtained (solid line) using $H_{el} = 100$ cm^{-1} along with experimental data points is shown in Figure 7, with good agreement between the two. The H_{el} value used for the fit is less than k_BT, suggesting that the electron transfer between TPA and Cu^{2+} shown in Scheme 1 is nonadiabatic and proceeds by an outer-sphere mechanism. Since $-\Delta G^0 \ll \lambda$ for the cases studied, the data points fall in the lower part of the normal region of the Marcus parabola.

For photoinduced electron-transfer reactions between organic donors and acceptors, the reorganization energy generally is in the range of 25–35 kcal M^{-1} and, hence, the value of 48.4 kcal M^{-1} obtained for the TPA/Cu^{2+} systems seems to be very high.[32] The high λ value is attributed to the high internal reorganization energy associated with the Cu^{2+}/Cu^{+} redox reaction. Cu^{2+} is a d^9 system and adopts a distorted-octahedral type six-coordinate geometry or a square pyramidal or trigonal bipyramidal type five-coordinate geometry. Cu^{+}, on the other hand, is a d^{10} system and adopts a four-coordinate tetrahedral geometry.[33,34] Thus, the reduction of Cu^{2+} to Cu^{+} would involve the rupture of one- or two-coordinate bonds and a change of the remaining bond angles. Equation 12 is based on the assumption that no chemical bonds are broken or formed during the electron-transfer process. Since bond rupture or formation is involved in the Cu^{2+}/Cu^{+} redox process, some researchers have questioned the validity of applying the Marcus equation to Cu^{2+}/Cu^{+} reactions.[35,36] However, the Marcus equation has been successfully applied to a large number of Cu^{2+}/Cu^{+} electron-transfer reactions[37] and, hence, we believe that the same can be done in the case of the TPA/Cu^{2+} electron-transfer reactions.

In $Cu(ClO_4)_2$ hexahydrate, the Cu^{2+} is bonded to six water molecules in a distorted octahedral geometry.[38] Four of the Cu–OH_2 bond lengths are nearly equal (~1.96 Å) while the other two are substantially larger (2.388 Å). When dissolved in ACN, the complex most probably exists as $[Cu(OH_2)_n(ACN)_{6-n}]^{2+}$ ($n = 0-3$) with $[Cu(OH_2)_2(ACN)_4]^{2+}$ as the dominant species in 99% ACN.[39] The Cu–ACN bond length in $[Cu(OH_2)_2(ACN)_4]^{2+}$ is 1.975 Å.[39] Electron transfer from TPA leads to formation of $[Cu(ACN)_4]^{+}$, which contains four acetonitrile molecules arranged in a tetrahedral fashion around the Cu^{+} (average bond angle of 109.4° and average Cu–N bond length of 1.99 Å).[40] Note that the Cu–ACN bond lengths do not change much during the electron-transfer process.[39] On the basis of these factors, we suggest the scheme in Figure 8 for electron transfer in the TPA/Cu^{2+} systems.

The precursor complex is shown in the left, the transition state is shown in the middle, and the successor complex is shown in the right. Upon proceeding from the precursor complex to the transition state, the Cu–OH_2 bonds weaken and the Cu–ACN bond angles change. Following electron transfer, the two Cu–OH_2 bonds are cleaved and the Cu–ACN bonds assume tetrahedral geometry in the successor complex, which subsequently dissociates into the products $TPA^{\bullet+}$ and $Cu(ACN)_4^{+}$. Since the electron transfer involves breaking of bonds and changing bond angles, the internal reorganization energy would be very high. In an attempt to determine if the λ obtained is reasonable, this value was used to estimate the reorganization energy for the Cu^{2+}/Cu^{+} self-exchange reaction ($\lambda_{Cu^{2+}/Cu^{+}}$) and compared to values from the literature.

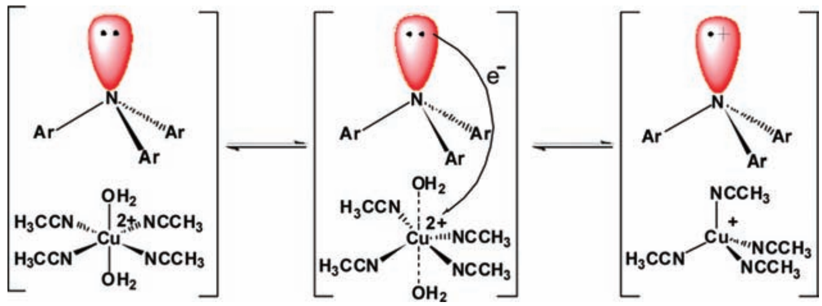

Figure 8. Schematic diagram of the electron-transfer process in the TPA/Cu^{2+} system.

Reorganization energies for self-exchange reactions can be obtained using eq 9, if rate constants for self-exchange reactions are known. Because of the high reorganization energy, aquacopper(II/I) and acetonitrilecopper(II/I) self-exchange reactions are extremely slow and difficult to study directly and indirect techniques are often used to estimate rate constants of these reactions.[37] Irangu et al. recently estimated a value of 4.0 × 10^{-8} M^{-1} s^{-1} for the self-exchange rate constant ($k_{Cu^{2+}/Cu^{+}}$) for Cu^{2+}/Cu^{+} in 100% ACN.[39] Substituting this value in eq 9, we obtained $\Delta G^* = 25$ kcal M^{-1} (assuming $Z = 10^{11}$ M^{-1} s^{-1}). Since $\Delta G^0 = 0$ for the self-exchange reaction, $\lambda_{Cu^{2+}/Cu^{+}} = 4 \times \Delta G^* = 100$ kcal M^{-1}, which is a very high value compared to that of other metal ions.[41] This value can be used to obtain a theoretical estimate of the reorganization energy for the TPA/Cu^{2+} reaction using the cross relationship in eq 13.

$$\lambda_{TPA/Cu^{2+}} = (1/2)(\lambda_{TPA/TPA^{\bullet+}} + \lambda_{Cu^{2+}/Cu^{+}}) \qquad (13)$$

where $\lambda_{TPA/TPA^{\bullet+}}$ is the reorganization energy for the TPA/$TPA^{\bullet+}$ self-exchange reaction. It is difficult to study intermolecular TPA/$TPA^{\bullet+}$ self-exchange reactions, but reorganization energy for the same can be calculated using standard equations. $\lambda_{TPA/TPA^{\bullet+}}$ has contributions from λ_i and λ_o. The λ_i contribution was calculated previously from the energies of the neutral and radical cation forms of TPA using AM1(UHF) and BPW1-DFT calculations, and the value obtained was 3.23 kcal M^{-1}.[42] The small value of λ_i indicates that the geometric change associated with radical cation formation is very small. λ_o can be calculated using eq 14.

$$\lambda_o = \Delta e^2(2r_1^{-1} + 2r_2^{-1} - d^{-1})(\varepsilon_{op}^{-1} - \varepsilon_s^{-1}) \qquad (14)$$

In eq 14, r_1 and r_2 refer to the radii of TPA and $TPA^{\bullet+}$, d is the center-to-center distance, and ε_{op} and ε_s are the optical and static dielectric constants of the solvent, acetonitrile. Since the geometric change associated with radical cation formation is very small, we can assume that $r_1 \approx r_2$. The radius of TPA obtained from AM1 is 5.3 Å. Taking $d = r_1 + r_2$, we obtain $\lambda_o = 16.54$ kcal M^{-1}. Thus, these calculations gave $\lambda_{TPA/TPA^{\bullet+}} = 19.77$ kcal M^{-1}. Substituting in eq 13, we get $\lambda_{TPA/Cu^{2+}} = 59.89$ kcal M^{-1}, which is about 20% higher than the value we obtained from fitting our kinetic data (Figures 5−7). It is to be noted that for the aquacopper(II/I) self-exchange reaction, estimated $k_{Cu^{2+}/Cu^{+}}$ values varied in the range of 1.9 × 10^{-4}−5.4 × 10^{-7} M^{-1} s^{-1}.[43−47] If we use these $k_{Cu^{2+}/Cu^{+}}$ values in eq 9, $\lambda_{Cu^{2+}/Cu^{+}}$ values in the range of 39.7−94.3 kcal M^{-1} are obtained. On the basis of the Born−Oppenheimer molecular dynamic simulation studies, Blumberger has recently suggested that the reorganization free energies for Cu^{+} and Cu^{2+} are asymmetric and differ by 1.0 eV.[48] $\lambda_{Cu^{2+}/Cu^{+}}$ estimated from this study was 3.9 eV (89.9 kcal M^{-1}). While these studies disagree on the actual value of $k_{Cu^{2+}/Cu^{+}}$, they all show that the self-exchange rate constant is exceptionally small in the aquacopper(II/I) system due to the large reorganization energy associated with the reaction. It is important to emphasize that our study also shows the involvement of large reorganization energy in the Cu^{2+}/Cu^{+} redox reaction.

4. Conclusions

We have studied the kinetic aspects of the electron-transfer reaction between TPA and Cu^{2+} in acetonitrile as a function of the driving force and temperature. The second-order rate constants exhibited a dependence on the ΔG^0 values and varied in the range of 1.02 × 10^2−2.15 × 10^5 M^{-1} s^{-1} when ΔG^0 was varied from +3.67 to −8.56 kcal M^{-1}. From the temperature dependence studies, the activation parameters for the reactions were determined. The reorganization energy estimated using experimental ΔG^* values is rather high. The experimental rate constants fit well to the Marcus equation which confirms the involvement of an outer-sphere electron transfer taking place in this reaction. The high reorganization energy is consistent with the cleavage of Cu−OH_2 bonds in the transition state, and a mechanism consistent with these observations is proposed.

Acknowledgment. We thank the Council of Scientific and Industrial Research (CSIR), Government of India, Department of Science and Technology (DST), Government of India (DST Project Numbers SR/S5/OC-15/2003 and DST/INT/NSF/RPO-230/2006), and the National Science Foundation (CHE-0413845) for financial support. We thank Mr. James Devery and Dr. Dhandapani V. Sadasivam for assistance with the stopped flow experiments. K.S. and C.V.S. thank CSIR for the research fellowship. This is contribution number NIIST-PPG-278.

References and Notes

(1) Das, S.; Suresh, V. In *Electron Transfer in Chemistry*; Balzani, V., Ed.; Wiley-VCH: New York, 2001; Vol. 2, pp 379−456.

(2) Fox, M. A., Chanon, M., Eds. *Photoinduced Electron Transfer*; Elsevier: Amsterdam, The Netherlands, 1988; Parts A−D.

(3) Kavarnos, G. J.; Turro, N. *J. Chem. Rev.* **1986**, *86*, 401.

(4) Theys, R. D.; Sosnovsky, G. *Chem. Rev.* **1997**, *97*, 83.

(5) Pullen, G. K.; Allen, N. S.; Edge, M.; Weddell, I.; Swart, R.; Catalina, F.; Navaratnam, S. *Eur. Polym. J.* **1996**, *32*, 943.

(6) Fiedler, D. A.; Koppenol, M.; Bond, A. M. *J. Electrochem. Soc.* **1995**, *142*, 862.

(7) Gerson, F.; Gescheidt, G.; Knöbel, J.; Martin, W. B., Jr.; Neumann, L.; Vogel, E. *J. Am. Chem. Soc.* **1992**, *114*, 7107.

(8) Gescheidt, G.; Herges, R.; Neumann, H.; Heinze, J.; Wollenweber, M.; Etzkorn, M.; Prinzbach, H. *Angew. Chem., Int. Ed. Engl.* **1995**, *34*, 1016.

(9) For a recent a review, see: Davies, A. G. *J. Chem. Res. Synop.* **2001**, 253.

(10) Krishna, R. M.; Chang, Z.; Choo, H.; Ranjit, K. T.; Kevan, L. *Phys. Chem. Chem. Phys.* **2000**, *2*, 3335.

(11) García, H.; Martí, V.; Casades, I.; Fornés, V.; Roth, H. D. *Phys. Chem. Chem. Phys.* **2001**, *3*, 2955.
(12) Folgado, J.-V.; Garcia, H.; Marti, V.; Esplá, M. *Tetrahedron* **1997**, *53*, 4947.
(13) Sumalekshmy, S.; Gopidas, K. R. *Chem. Phys. Lett.* **2005**, *413*, 294.
(14) Kirchgessner, M.; Sreenath, K.; Gopidas, K. R. *J. Org. Chem.* **2006**, *71*, 9849.
(15) Sreenath, K.; Suneesh, C. V.; Ratheesh Kumar, V. K.; Gopidas, K. R. *J. Org. Chem.* **2008**, *73*, 3245.
(16) Rosokha, S. V.; Kochi, J. K. *Acc. Chem. Res.* **2008**, *41*, 641.
(17) Wu, A.; Mayer, J. M. *J. Am. Chem. Soc.* **2008**, *130*, 14745.
(18) Chen, X.; Brauman, J. I. *J. Am. Chem. Soc.* **2008**, *130*, 15038.
(19) Enemærke, R. J.; Hertz, T.; Skrydstrup, T.; Daasbjerg, K. *Chem. Eur. J.* **2000**, *6*, 3747.
(20) Enemærke, R. J.; Daasbjerg, K.; Skrydstrup, T. *Chem. Commun.* **1999**, 343.
(21) Armstrong, D. A.; Sun, Q.; Schuler, R. H. *J. Phys. Chem.* **1996**, *100*, 9892.
(22) Baggott, J. E. In *Photoinduced Electron Transfer*; Fox, M. A., Channon, M., Eds.; Elsevier: New York, 1988; Part B.
(23) Kavarnos, G. J. *Fundamentals of Photoinduced Electron Transfer*; VCH: New York, 1993.
(24) Prasad, E.; Flowers, R. A., II. *J. Am. Chem. Soc.* **2002**, *124*, 6357.
(25) Dahlén, A.; Hilmersson, G. *J. Am. Chem. Soc.* **2005**, *127*, 8340.
(26) Marcus, R. A. *Faraday Discuss. Chem. Soc.* **1982**, *74*, 7.
(27) Marcus, R. A.; Sutin, N. *Biochim. Biophys. Acta* **1985**, *811*, 265.
(28) Sutin, N. *Acc. Chem. Res.* **1982**, *15*, 275.
(29) Marcus, R. A. *Angew. Chem., Int. Ed. Engl.* **1993**, *32*, 1111.
(30) Bock, C. R.; Connor, J. A.; Gutierrez, A. R.; Meyer, T. J.; Whitten, D. G.; Sullivan, B. P.; Nagle, J. K. *J. Am. Chem. Soc.* **1979**, *101*, 4815.
(31) Fukuzumi, S.; Wong, C. L.; Kochi, J. K. *J. Am. Chem. Soc.* **1980**, *102*, 2928.
(32) Gould, I. R.; Farid, S. *Acc. Chem. Res.* **1996**, *29*, 522.
(33) Hathaway, B. J.; Billing, D. E. *Coord. Chem. Rev.* **1970**, *5*, 143.
(34) Hathaway, B. J. *Coord. Chem. Rev.* **1981**, *35*, 211.
(35) Lee, C.-W.; Anson, F. C. *J. Phys. Chem.* **1983**, *87*, 3360.
(36) Lee, C.-W.; Shin, D. S.; Chair, T. S.; Kim, K. *Bull. Korean Chem. Soc.* **1991**, *12*, 454.
(37) Rorabacher, D. B. *Chem. Rev.* **2004**, *104*, 651.
(38) Gallucci, J. C.; Gerkin, R. E. *Acta Crystallogr.* **1989**, *C45*, 1279.
(39) Irangu, J.; Ferguson, M. J.; Jordan, R. B. *Inorg. Chem.* **2005**, *44*, 1619.
(40) Csöregh, I.; Kierkegaard, P.; Norrestam, R. *Acta Crystallogr.* **1975**, *B31*, 314.
(41) Marcus, R. A. *Rev. Mod. Phys.* **1993**, *65*, 599.
(42) Low, P. J.; Paterson, M. A. J.; Yufit, D. S.; Howard, J. A. K.; Cherryman, J. C.; Tackley, D. R.; Brook, R.; Brown, B. *J. Mater. Chem.* **2005**, *15*, 2304.
(43) Hoselton, M. A.; Lin, C.-T.; Schwarz, H. A.; Sutin, N. *J. Am. Chem. Soc.* **1978**, *100*, 2383.
(44) Davies, K. M. *Inorg. Chem.* **1983**, *22*, 615.
(45) Sisley, M. J.; Jordan, R. B. *Inorg. Chem.* **1992**, *31*, 2880.
(46) Gaunder, R. G.; Taube, H. *Inorg. Chem.* **1970**, *9*, 2627.
(47) Manahan, S. E. *Can. J. Chem.* **1967**, *45*, 2451.
(48) Blumberger, J. *J. Am. Chem. Soc.* **2008**, *130*, 16065.

JP9027222